View Article Online
View Journal

Journal of Materials Chemistry A

Materials for energy and sustainability

Accepted Manuscript

This article can be cited before page numbers have been issued, to do this please use: L. Wang, B. Zhao, C. Wang, M. Sun, Y. Yu and B. Zhang, *J. Mater. Chem. A*, 2020, DOI: 10.1039/D0TA01256D.

Volume 6
Number 12
28 March 2018
Pages 4883-5230

Journal of Materials Chemistry A

Materials for energy and sustainability

rsc.li/materials-a

ISSN 2050-7488

ROYAL SOCIETY OF CHEMISTRY

COMMUNICATION
Zhenhai Wen *et al.*
An electrochemically neutralized energy-assisted low-cost acid-alkaline electrolyzer for energy-saving electrolysis hydrogen generation

View Article Online
DOI: 10.1039/D0TA01256D

Journal Name

COMMUNICATION

Thermally-Assisted Photocatalytic Conversion of CO_2-H_2O to C_2H_4 over Carbon Doped In_2S_3 Nanosheets

Lei Wang,‡[a] Bohang Zhao,‡[a] Changhong Wang,[a] Mengyao Sun,[a] Yifu Yu[a] and Bin Zhang*[ab]

Received 00th January 20xx,
Accepted 00th January 20xx

DOI: 10.1039/x0xx00000x

www.rsc.org/

The development of an efficient photocatalyst for selective conversion of CO_2 to ethylene (C_2H_4) is highly desirable. Here, carbon-doped In_2S_3 nanosheet-based spheres (denoted as C-In_2S_3) are reported to be highly efficient for thermal-assisted photocatalytic conversion of CO_2-H_2O to C_2H_4 at 150 °C without any cocatalysts or sacrificial agents. The total consumed electron number (TCEN) for CO_2 conversion over C-In_2S_3 can reach 472.7 $\mu mol\ g^{-1}\ h^{-1}$. The selectivity and production rate of C_2H_4 over C-In_2S_3 are about 50 % and 26.6 ± 4.1 $\mu mol\ g^{-1}\ h^{-1}$, respectively, with a quantum efficiency of 13.3 % at 420 nm. Meanwhile, no C_2H_4 can be detected over In_2S_3 without carbon doping. $^{13}CO_2$ and D_2O isotope labeling experiments confirm the carbon and hydrogen origins of C_2H_4. In situ experimental and theoretical studies reveal that carbon doping accelerates CO_2 adsorption and activation, lower the energy barrier to form CH*, the key intermediates for C_2H_4, thus leading to high selectivity.

The continuous consumption of fossil fuels has caused intensive environmental issues and concerns.[1-4] To relieve the greenhouse effect, the use of solar-driven photocatalytic technology to convert carbon dioxide into fuels and useful chemicals has become one of the very promising strategies.[5-12] However, the thermodynamical stability of CO_2 and the slow kinetics of multiple carriers transfer processes made the photocatalytic conversion of CO_2 (CO_2-PC) be of low efficiency.[13-17] Recently, the thermally-assisted photocatalytic strategy has been developed to accelerate CO_2-PC.[18-22] Most cases needed H_2, which is commercially produced from steam reforming of fossil derivates with CO_2 emission. So, directly using water as hydrogen sources is urgently needed. But at present, the main products for CO_2-PC are CO and CH_4,[23-28] and high-value C_2 species are still difficult to be synthesized. Ethylene is the most important C_2 chemical because of the wide use in the synthesis of synthetic fibers, rubbers, plastics, and alcohol.[29-30] Typically, ethylene is synthesized by methanol-to-olefins process or thermal steam cracking of petroleum,[31-33] which requires high temperature and suffers severe catalyst coking problems. Therefore, it is highly desirable to develop an efficient photocatalyst for selectively converting CO_2 and H_2O to ethylene.

Element doping is an effective strategy to modify the electronic property and surface structure of semiconductors with improved performances.[34-36] For instance, element doping can change the diffusion path of carriers.[36] Non-metal doping can broaden the light absorption range and reduce the light corrosion.[37] And the doped element can act as a good electron acceptor center and effectively inhibit the recombination of charge carriers.[38] Thus, doping none metal into one semiconductor photocatalyst for synthesizing ethylene from the conversion of CO_2-H_2O is of great interest.

Herein, we only used a facile hydrothermal treatment of the organic-inorganic hybrid InS-TETA precursor to prepare carbon-doped In_2S_3 nanosheet-based spheres (denoted as C-In_2S_3, (see Supporting Information for details†)). C-In_2S_3 is demonstrated as an efficient photocatalyst for selectively converting CO_2-H_2O to C_2H_4 at 150 °C in the absence of any sacrificial agents or cocatalysts. The combined results of *in situ* diffuse reflectance infrared Fourier transform spectroscopy (DRIFTS) and density functional theory (DFT) simulation reveal that the doping of carbon into In_2S_3 lattice can decrease the transformation energy barriers from CO_2 to CO and then from

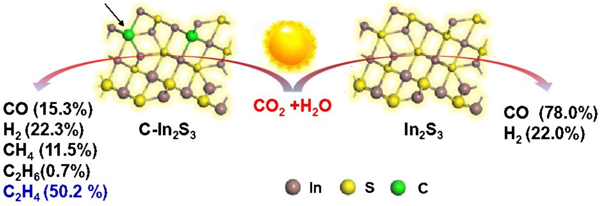

Fig. 1 Schematic diagram illustrating the distribution of the products via thermally-assisted photocatalytic conversion of CO_2-H_2O over In_2S_3 and C-In_2S_3.

---

[a] Department of Chemistry, School of Science, Institute of Molecular Plus, Tianjin University, Tianjin 300072, China
[b] Tianjin Key Laboratory of Molecular Optoelectronic Sciences, Tianjin University, Tianjin 300072, China

†Electronic Supplementary Information (ESI) available: Experimental details, supplementary characterization and electrochemical measurements. See DOI: 10.1039/x0xx00000x

‡ The authors contributed equally.

View Article Online
DOI: 10.1039/D0TA01256D

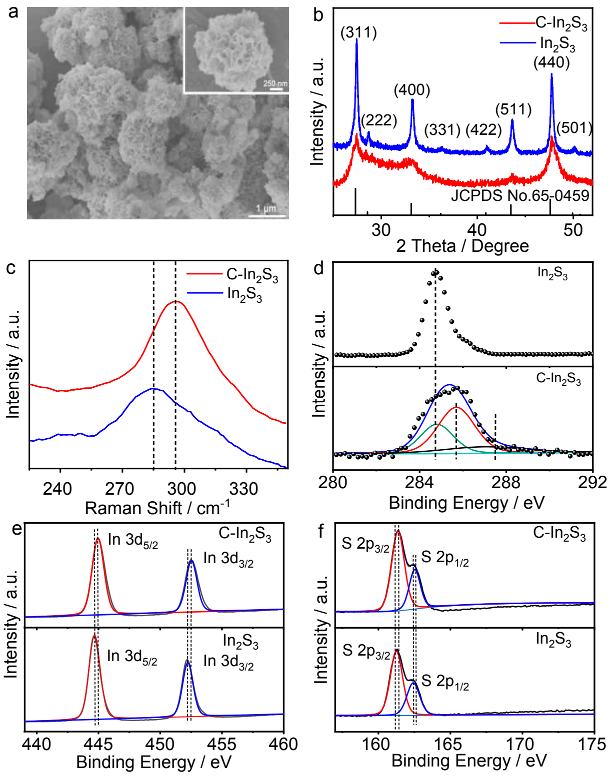

Fig. 2 (a and inset) SEM images of C-In$_2$S$_3$. (b) XRD patterns of C-In$_2$S$_3$ and In$_2$S$_3$. (c) Raman spectra of C-In$_2$S$_3$ and In$_2$S$_3$. (d-f) High-resolution XPS spectra of (d) C 1s, (e) S 2p and (f) In 3d of C-In$_2$S$_3$ and In$_2$S$_3$.

CO to CH* species, one of the important intermediates for the exothermal formation of CH$_2$* and C$_2$H$_4$.

In$_2$S$_3$ samples with and without carbon doping were synthesized according to the modified L-cysteine-assisted hydrothermal method and solid-phase reactions, respectively (see the Supporting Information for details). Scanning electron microscopy (SEM) and transmission electron microscopy (TEM) images (Fig. 2a and Fig. S1a†, S2a†,b†) show that both C-In$_2$S$_3$ and In$_2$S$_3$ are hierarchical spheres composed of nanosheets. In the corresponding high-resolution TEM (HRTEM) images (Fig. S1b†, S2c†), the lattice spacing of 0.328 nm indexed to the (311) plane of In$_2$S$_3$ is smaller than that of C-In$_2$S$_3$, which is in agreement with the reported carbon-doped SnS$_2$.[39] All the X-ray diffraction (XRD) peaks are ascribed to cubic In$_2$S$_3$ (JCPDS NO. 65-0459) (Fig. 2b). Compared with In$_2$S$_3$, the peak of C-In$_2$S$_3$ is wider and weaker, indicating that carbon doping reduced the order of the lattice (Fig. S1b†). In comparison with pure In$_2$S$_3$, the Raman characteristic peak of In$_2$S$_3$ in C-In$_2$S$_3$ experiences a positive shift of about 9 cm^{-1} (Fig. 2c), resulting from the inter-layer covalent interaction after carbon doping.[40] Also, the Raman spectra (Fig. S3†) confirms the existence of carbon in C-In$_2$S$_3$ and the absence of any carbonaceous materials in In$_2$S$_3$. In C 1s X-ray photoelectron spectroscopy (XPS) spectra (Fig. 2d), C-In$_2$S$_3$ owns a broader peak than In$_2$S$_3$, which can be divided into three peaks ascribed to adventitious carbon (sp$_3$ C-C, 284.8 eV), sp$_3$-coordinated carbon bonds from the defects in the In$_2$S$_3$ (C$_{intercalation}$, 285.8 eV) and substituting carbon with lattice sulfur (C-S, 287.3 eV), respectively. Such interaction of carbon and sulfur further confirms the doping of carbon in C-In$_2$S$_3$.[41-42] Furthermore, the binding energy of In and S in C-In$_2$S$_3$ shift positively due to the distortion of the lattice caused by doping carbon (Fig. 2e, f).[37] It can be seen from the XPS spectra that the intensity of the N 1s peak is almost same in both samples, but C-In$_2$S$_3$ has a stronger C 1s peak than In$_2$S$_3$ (Fig. S4†). The signals for N might origin from the XPS chamber during the measurements. So, the effect of N doping can be usually neglected.[39] All these results suggest that In$_2$S$_3$ with and without carbon doping are synthesized successfully.

The thermally-assisted photocatalytic conversion of CO$_2$-H$_2$O was performed under the illumination of 300 W Xe lamp with external heat (see Supporting Information for details†). As shown in Fig. 3a, the main products over In$_2$S$_3$ are H$_2$ (121.5 ± 18.2 μmol g^{-1}) and CO (34.2 ± 9.7 μmol g^{-1}) without any alkanes and olefins. But for the prepared C-In$_2$S$_3$, the production amount of C$_2$H$_4$ can reach 133.0 ± 20.5 μmol g^{-1}. The selectivity of C$_2$H$_4$ is about 50.2 % among all gaseous products, and 80.3 % among hydrocarbon products, illustrating that the doping of carbon can suppress the hydrogen evolution and promote the C-C coupling. Meanwhile, the amount of all products over C-In$_2$S$_3$ shows time-dependent growth with a high evolving rate of C$_2$H$_4$ (26.6 ± 4.1 μmol g^{-1} h^{-1}) and a quantum efficiency of 13.3 % at 420 nm (Fig. 3b). In general, the total consumed electron number (TCEN) for CO$_2$ conversion is often used to estimate CO$_2$ reduction efficiency due to the complexity of the products. The TCEN of C-In$_2$S$_3$ was higher than other photocatalysts (Table S1). Furthermore, no obvious deactivation is observed after 5 cycles and to check the carbon for loss on C-In$_2$S$_3$ photocatalyst (Fig. 3c), the chemical compositions of C-In$_2$S$_3$ after five consecutive cycles were added to the Tables S2,S3. The results show little loss of carbon was found after tests, confirming the good stability of C-In$_2$S$_3$ for converting CO$_2$-H$_2$O to C$_2$H$_4$. Its high morphology and structure stability are further confirmed by the SEM, HRTEM and XPS results after consecutive runs (Fig. S5†). Then, to investigate the light-driven photocatalytic reaction of CO$_2$-H$_2$O, a series of control experiments are carried out. Firstly, when the H$_2$O was replaced by H$_2$ without light and other conditions remain unchanged, the main product was CO, rather than C$_2$H$_4$, indicating that the formation process of C$_2$H$_4$ is driven by light illumination. Next, we explored the temperature-dependent performance. The photocatalytic conversion performance of CO$_2$ is poor without external heat (Table S4 and Fig. S6†). As shown in Fig. S6a†, the high temperature can indeed promote the formation of C$_2$H$_4$. But for the photocatalytic CO$_2$-H$_2$O over C-In$_2$S$_3$, a higher test temperature might lead to the changes in the morphology and structure of the sample. After five cycles measurements at 180 °C, we also observe the morphology change of C-In$_2$S$_3$ samples with a decreasing performance (Fig. S6a† and Fig. S7†), which may be the possible oxidation at elevated temperature. Thus, to maintain the stability of the sample morphology and structure, the test temperature of 150 °C was selected at the

View Article Online
DOI: 10.1039/D0TA01256D

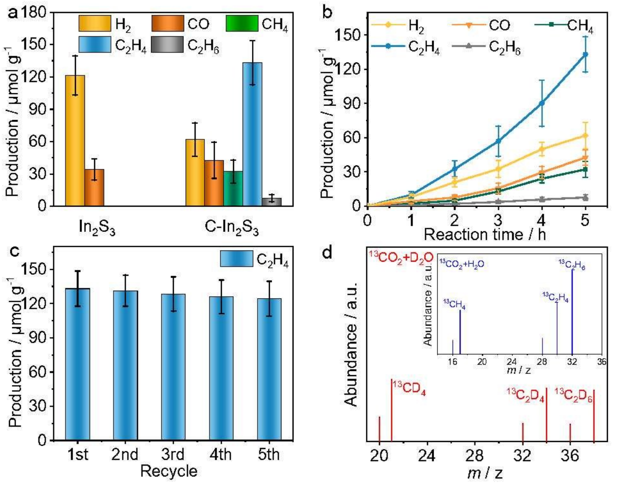

Fig. 3 (a) Performance comparison of C-In_2S_3 and In_2S_3 under UV-Visible light at 150 °C for 5 h. (b) Production amount of H_2, CO, CH_4, C_2H_4, and C_2H_6 as a function of reaction time over C-In_2S_3. (c) Stability test of C-In_2S_3 (5 hr for one cycle). d and inset) Mass spectra of $^{13}CO_2$-D_2O and $^{13}CO_2$-H_2O isotope experiments over C-In_2S_3

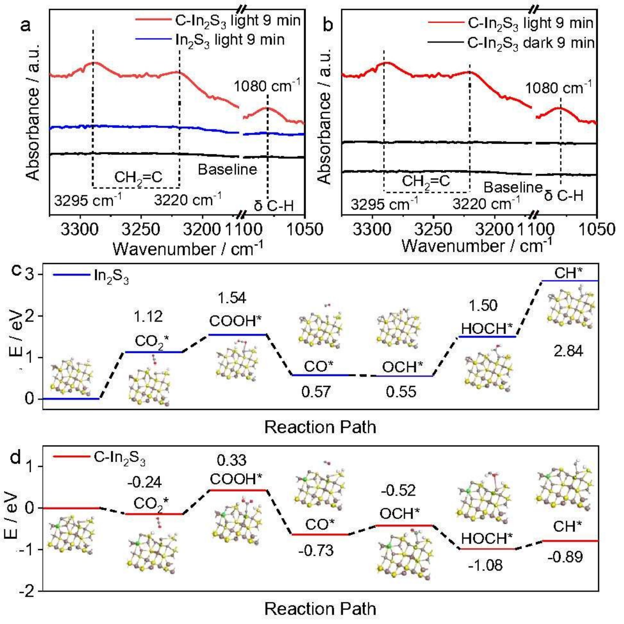

Fig. 4 (a) *In situ* DRIFTS spectra for CO_2-H_2O over C-In_2S_3 and In_2S_3 illuminated for 9 minutes. (b) *In situ* DRIFTS spectra for CO_2-H_2O over C-In_2S_3 in the dark and under 9 minutes' illumination. Calculated reaction energy diagrams of CO_2 to CH* over the H-terminated surface of (c) In_2S_3 and (d) C-In_2S_3.

optimal temperature here. O_2 can also be detected at room temperature (Fig. S8†). To investigate whether there are other oxidation products in the product, we performed the XPS spectra for a survey scan of C-In_2S_3 (Fig. S9†), we found that the O 1s peak of the sample did not change significantly before and after five consecutive cycles, which confirmed that there were no other oxidation products except for O_2, suggesting that the photocatalytic water splitting provides hydrogen source for C_2H_4 and the water acts as the electron donor. These results reveal that the conversion of CO_2-H_2O to C_2H_4 is a thermally-assisted photocatalytic process. To verify the carbon and hydrogen sources of C_2H_4, $^{13}CO_2$ and D_2O isotope tracing experiments are performed (Fig. 3d). When CO_2 is replaced by $^{13}CO_2$, $^{13}CH_4$ ($m/z = 17$)、$^{13}C_2H_4$ ($m/z = 30$)、$^{13}C_2H_6$ ($m/z = 32$) are detected, indicating that the carbon atoms of C_2H_4 are derived from CO_2. Furthermore, when H_2O is substituted by D_2O, $^{13}CD_4$ ($m/z = 21$)、$^{13}C_2D_4$ ($m/z = 34$)、$^{13}C_2D_6$ ($m/z = 38$) are detected, implying that the H atoms of C_2H_4 are derived from H_2O.

To get insight into the reason why C_2H_4 can be effectively produced over C-In_2S_3 during the thermally-assisted photocatalytic conversion of CO_2-H_2O, *in situ* diffuse reflectance infrared Fourier transform spectroscopy (DRIFTS) were utilized in a continuous steam-saturated carbon dioxide flow. With the irradiated time increasing, the intensity of in-plane deformation vibration of δ_{C-H} in hydrocarbon intermediates at 1080 cm^{-1} is enhanced over C-In_2S_3.[43] Also, there is a quick growth of the peaks at 3220 and 3295 cm^{-1} that are attributed to the stretching vibrations of C-H on unsaturated *CH_2=C (Fig. S10†), one of the important intermediates for forming C_2H_4.[44-45] Whereas, there are no obvious signals of hydrocarbon intermediates over In_2S_3 under the same conditions (Fig. 4a). Besides, when such conversion experiments are carried out over C-In_2S_3 in a dark circumstance with other conditions remaining unchanged, any signals of δ_{C-H} and *CH_2=C cannot be detected (Fig. 4b). These *in situ* DRIFTS further confirm the doping of carbon is significant to produce C_2H_4 during the photocatalytic process. To further understand the formation mechanism of C_2H_4 over C-In_2S_3, the spin-polarized first-principles calculations based on the density functional theory (DFT) was performed (Fig. S11 †).[46-47] As shown in Fig. S12†, the water adsorption and dissociation to H* processes are easier to occur on the surface of C-In_2S_3, indicating that the H-terminated surface over C-In_2S_3 is easier to form. It is widely accepted that the formation of C_2H_4 often involves two steps: 1) CO_2 adsorption and subsequent conversion from CO_2 to CO; 2) hydrogenation and subsequent coupling of adsorbed CO.[48-51] So, we simulate the two processes over H-terminated surfaces of C-In_2S_3 and In_2S_3. As shown in Fig. 4d, the adsorption energy of CO_2 on C-In_2S_3 is -0.24 eV, which is much lower than that on In_2S_3 (1.12 eV) (Fig. 4c, d). The next two steps involving CO_2* to COOH* transformation and CO* generation are energetically similar on the two surfaces of In_2S_3 and C-In_2S_3, suggesting the superiority of carbon doping on CO_2 activation. Furthermore, CO* can be easily hydrogenated to form OCH* on both In_2S_3 and C-In_2S_3, respectively. However, the reaction Gibbs free energies from OCH* to HOCH* and from HOCH* to CH* on C-In_2S_3 are -0.56 and 0.19 eV, respectively, which are much lower than those on the In_2S_3 (0.95 and 1.34 eV), indicating that OCH* can be further hydrogenated to form CH* on C-In_2S_3, supporting the *in situ* DRIFTS observation. At last, the evolved process of CH*→CH_2*→C_2H_4 is exothermal and beneficial to reduce the number of free radicals (Fig. S13†). The combined *in situ* DRIFTS and DFT results reveal that the doping of carbon into In_2S_3 lattice can enhance the adsorption and activation of H_2O and CO_2, and lower the energy barriers for

View Article Online
DOI: 10.1039/D0TA01256D

promoting the formation of hydrocarbon intermediates, thus leading to the high selectivity of C_2H_4 over C-In_2S_3.

The UV-Vis diffuse reflectance spectra (Fig. S14†), ultraviolet photoemission spectra (UPS) (Fig. S15†), and their derived band structure (Fig. S16 †) suggest that both the reductive and oxidative ability of catalysts can be enhanced after carbon doping, benefiting the multi-electron reduction process.[37, 52-54] Moreover, the photoluminescence (PL) data (Fig. S17 †) indicates that the photoinduced carriers recombination is greatly suppressed after the doping of carbon.[55-57]

Conclusions

In summary, we demonstrated carbon-doped In_2S_3 as an efficient and durable photocatalyst for synthesizing C_2H_4 via the thermally-assisted photocatalytic conversion of CO_2-H_2O, in which water is directly used as hydrogen sources. In the absence of any sacrificial agents or cocatalysts, the production rate and selectivity of C_2H_4 can be reached to 26.6 ± 4.1 $\mu mol\ g^{-1}\ h^{-1}$ and 50.2 %. $^{13}CO_2$ and D_2O isotope tracing experiments confirm that the carbon and hydrogen atoms of C_2H_4 originate from CO_2 and H_2O, respectively. The in situ experimental and theoretical results reveal that doping carbon could not only enhance water adsorption/dissociation and CO_2 activation, but also decrease energy barriers of forming hydrocarbon intermediates for C_2H_4, thus resulting in high selectivity of C_2H_4. This work offers new opportunities to design constructions of carbon-doping photocatalysts for synthesizing value-added C_2 chemicals via thermally assisted photocatalytic conversion of CO_2-H_2O.

Conflicts of interest

The authors declare no competing financial interest.

Acknowledgements

We acknowledge the financial support from the National Natural Science Foundation of China (No. 21871206 and No. 21422104) and the Natural Science Foundation of Tianjin City (No. 17JCJQJC44700).

Notes and references

1 M. Schreier, F. Héroguel, L. Steier, S. Ahmad, J. S. Luterbacher, M. T. Mayer, J. Luo and M. Grätzel, *Nat. Energy,* 2017, **2,** 17087.
2 M. Marszewski, S. Cao, J. Yu and M. Jaroniec, *Mater. Horiz.,* 2015, **2,** 261-278.
3 J. Ran, M. Jaroniec and S. Z. Qiao, *Adv. Mater.* 2018, **30,** 1704649.
4 G. A. Ozin, *Adv. Mater.* 2015, **27,** 1957-1963.
5 D. B. Burks, S. Davis, R. W. Lamb, X. Liu, R. R. Rodrigues, N. P. Liyanage, Y. Sun, C. E. Webster, J. H. Delcamp and E. T. Papish, *Chem. Commun.,* 2018, **54,** 3819-3822.
6 K. Li, B. Peng and T. Peng, *ACS Catal.,* 2016, **6,** 7485-75277.
7 D. Chen, X. Zhang and A. Lee, *J. Mater. Chem. A,* 2015, **3,** 14487-14516.
8 D. L. Liu, Y. Xu, M. Y. Sun, Y. Huang, Y. F. Yu and B. Zhang, *J.Mater. Chem. A,* 2020, **8,** 1077-1083.
9 X. Zhang, X. Li, D. Zhang, N. Q. Su, W. Yang and H. O. Everitt, J. Liu, *Nat. Commun.,* 2017, **8,** 14542.
10 N. Meng, C. Liu, Y. Liu and B. Zhang, *Angew. Chem. Int. Ed.,* 2019, **58**, 18908-18912.
11 A. Zhang, Y. Liang, H. Li, X. Zhao, Y. Chen, B. Zhang, W. Zhu and J. Zeng, *Nano Lett.,* 2019, **19,** 6547-6553.
12 Y. X. Pan, Y. You, S. Xin, Y. Li, G. Fu, Z. Cui, Y. L. Men, F. F. Cao, S. H. Yu and Goodenough, J. B, *J. Am. Chem. Soc.,* 2017, **139,** 4123-4129.
13 C. Cometto, R. Kuriki, L. Chen, K. Maeda, T. C. Lau, O. Ishitani and M. Robert, *J. Am. Chem. Soc.,* 2018, **140,** 7437-7440.
14 B. M. Tackett, E. Gomez and J. G. Chen, *Nat. Catal.,* 2019, **2,** 381-386.
15 B. Zhao, Y. Huang, D. Liu, Y. Yu and B. Zhang, *Sci. China Chem.,* 2020, **63,** 28-34.
16 D. Gao, Y. Zhang, Z. Zhou, F. Cai, X. Zhao, W. Huang, Y. Li, J. Zhu, P. Liu, F. Yang, G. Wang and X. Bao, *J. Am. Chem. Soc.,* 2017, **139,** 5652-5655.
17 X. Cui, J. Wang, B. Liu, S. Ling, R. Long and Y. Xiong, *J. Am. Chem. Soc.,* 2018, **140,** 16514-16520.
18 M. Ghoussoub, M. Xia, P. N. Duchesne, D. Segal and G. A. Ozin, *Energy Environ. Sci.,* 2019, **12,** 1122-1142.
19 Z. J. Wang, H. Song, H. Liu and J. Ye, *Angew. Chem. Int. Ed.,* 2020, DOI: 10.1002/anie.201907443.
20 G. Chen, G. I. N. Waterhouse, R. Shi, J.Zhao, Z. Li, L. Z. Wu, C. H. Tung and T. Zhang, *Angew. Chem. Int. Ed.,* 2019, **58,** 17528-17551.
21 D. L. Liu, C. H. Wang, Y. F. Yu, B. H. Zhao, W. C. Wang, Y. H. Du and B. Zhang, *Chem,* 2019, **5,** 376-389.
22 Z. Sun, N. Talreja, H. Tao, J. Texter, M. Muhler, J. Strunk and J. Chen, *Angew. Chem. Int. Ed.,* 2018, **57,** 7610-7627.
23 S. Wang, B. Y. Guan and X. W. Lou, *J. Am. Chem. Soc.,* 2018, **140**, 5037-5040.
24 X. Yu, Z. Yang, B. Qiu, S. Guo, P. Yang, B. Yu, H. Zhang, Y. Zhao, X. Yang, B. Han and Z. Liu, *Angew. Chem. Int. Ed.,* 2019, **58,** 632-636.
25 X. Hong, J. Kim, S. F. Shi, Y. Zhang, C. Jin, Y. Sun, S. Tongay, J. Wu, Y. Zhang and F. Wang, *Nat. Nanotechnol.,* 2014, **9,** 682-686.
26 Y. Wang, Z. Zhang, L. Zhang, Z. Luo, J. Shen, H. Lin, J. Long, J. C. S. Wu, X. Fu, X. Wang and C. Li, *J. Am. Chem. Soc.,* 2018, **140,** 14595-14598.
27 C. Liu, B. C. Colón, M. Ziesack, P. A. Silver and D. G. Nocera, *Science,* 2016, **352,** 1210.
28 Q. Lu, Y. Yu, Q. Ma, B. Chen and H. Zhang, *Adv. Mater.,* 2016, **28,** 1917-1933.
29 L. Zhong, F. Yu, Y. An, Y. Zhao, Y. Sun, Z. Li, T. Lin, Y. Lin, X. Qi, Y. Dai, L. Gu, J. Hu, S. Jin, Q. Shen and H. Wang, *Nature,* 2016, **538,** 84-87.
30 X. Zhu, S. Jiang, C. Li, X. Chen and C. Yang, *Ind Eng. Chem. Res.,* 2013, **52,** 14366-14375.
31 X. B. Zhao, J. Z. Li, P. Tian, L. Y. Wang, X. F. Li, S. F. Lin, X. W. Guo and Z. M. Liu, *ACS Catal.,* 2019, **9,** 3017-3025.

View Article Online
DOI: 10.1039/D0TA01256D

32 P. Tian, Y. X. Wei, M. Ye and Z. M. Liu, *ACS Catal.,* 2015, **5,** 1922-1938.
33 Y. Gao, L. Neal, D. Ding, W. Wu, C. Baroi, A. M. Gaffney and F. Li, *ACS Catal.,* 2019, **9,** 8592-8621.
34 Y. Park, W. Kim, H. Park, T. Tachikawa, T. Majima and W. Choi, *Appl. Catal. B: Environ.,* 2009, **91,** 355-361.
35 F. E. Osterloh, *Chem. Soc. Rev.,* 2013, **42,** 2294-2320.
36 M. Zheng, J. Shi, T. Yuan and X. Wang, *Angew. Chem. Int. Ed.,* 2018, **57,** 5487-5491.
37 A. I. J. Joseph and S. Thiripuranthagan, *J. Nanosci Nanotechnol.,* 2018, **18,** 3158-3164.
38 K. Wang, Q. Li, B. S. Liu, B. Cheng, W. K. Ho and J. G. Yu, *Appl. Catal. B-Environ.,* 2015, **176,** 44-52.
39 I. Shown, S. Samireddi, Y. C. Chang, R. Putikam, P. H. Chang, A. Sabbah, F. Y. Fu, W. F. Chen, C. I. Wu, T. Y. Yu, P. W. Chung, M. C. Lin, L. C. Chen and K. H. Chen, *Nat. Commun.,* 2018, **9,** 169.
40 T. E. Doyle and J. R. Dennison, *Phys. Rev. B,* 1995, **51,** 196-200.
41 J. Fu, B. Zhu, C. Jiang, B. Cheng, W. You and J. Yu, *Small,* 2017, **13,** 1603938.
42 K. C. Pillai, V. Y. Young and J. O. M. Bockris, *Appl. Surf. Sci.,* 1983, **16,** 322-344.
43 D. A. Dows, *J. Chem. Phys.,* 1962, **36,** 2833-2835.
44 G. Fischer, R. E. Miller, P. F. Vohralik and R. O. Watts, *J. Chem. Phys.,* 1985, **83,** 1471-1477.
45 C. C. Wang, P. Zielke, O. F. Sigurbjornsson, C. R. Viteri and R. Signorell, *J. Phys. Chem. A,* 2009, **113,** 11129-11137.
46 S. J. Clark, M. D. Segall, C. J. Pickard, P. J. Hasnip, M. J. Probert, K. Refson and M. C. Payne, *Z. Kristallogr.,* 2005, **220,** 567-570.
47 E. R. McNellis and J. Meyer, K. Reuter, *Phys. Rev. B,* 2009, **80,** 205414.
48 W. Gao, R. Gao, Y. F. Zhao, M. Peng, C. Q. Song, M. Z. Li, S. W. Li, J. J. Liu, W. Z. Li, Y. C. Deng, M. T. Zhang, J. L. Xie, G. Hu, Z. S. Zhang, R. Long, X. D. Wen and D. Ma, *Chem,* 2018, **4,** 2917-2928.
49 Y. Wang, X. Zhu and Y. Li, *J. Phys. Chem. Lett.,* 2019, **10,** 4663-4667.
50 A. A. Peterson, F. Abild-Pedersen, F. Studt, J. Rossmeisl and J. K. Nørskov, *Energy Environ. Sci.,* 2010, **3,** 1311-1315.
51 Y. Jiao, Y. Zheng, P. Chen, M. Jaroniec and S. Z. Qiao, *J. Am. Chem. Soc.,* 2017, **139,** 18093-18100.
52 H. Ihara, H. Abe, S. Endo and T. Irie, *Solid State Commun.,* 1978, **28,** 563-565.
53 M. Xing, Y. Zhou, C. Dong, L. Cai, L. Zeng, B. Shen, L. Pan, C. Dong, Y. Chai, J. Zhang and Y. Yin, *Nano Lett.,* 2018, **18,** 3384-3390.
54 C. Dong, C. Lian, S. Hu, Z. Deng, J. Gong, M. Li, H. Liu, M. Xing and J. Zhang, *Nat. Commun.,* 2018, **9,** 1252.
55 X. Song, D. He, W. Li, Z. Ke, J. Liu, C. Tang, L. Cheng, C. Jiang, Z. Wang and X. Xiao, *Angew. Chem. Int. Ed.,* 2019, **58,** 16660-16667.
56 S. Chen, H. Wang, Z. Kang, S. Jin, X. Zhang, X. Zheng, Z. Qi, J. Zhu, B. Pan and Y. Xie, *Nat. Commun.,* 2019, **10,** 788.
57 J. Wang, T. Xia, L. Wang, X. Zheng, Z. Qi, C. Gao, J. Zhu, Z. Q. Li, H. Xu and Y. Xiong, *Angew. Chem. Int. Ed.,* 2018, **57,** 16447-16451.

View Article Online
DOI: 10.1039/D0TA01256D

Table of contents

Thermally-Assisted Photocatalytic Conversion of CO_2-H_2O to C_2H_4 over Carbon Doped In_2S_3 Nanosheets

Lei Wang,‡[a] Bohang Zhao,‡[a] Changhong Wang,[a] Mengyao Sun,[a] Yifu Yu[a] and Bin Zhang*[ab]

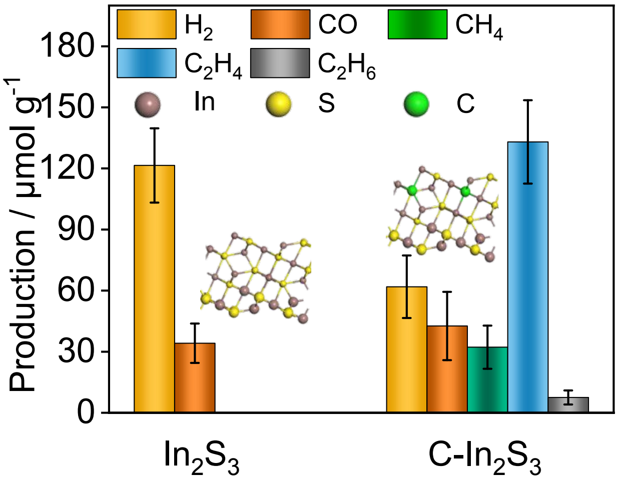

Carbon-doped In_2S_3 (C-In_2S_3) is a highly efficient photocatalyst for selectively converting CO_2-H_2O to C_2H_4 at 150 °C without any sacrificial agents or cocatalysts. The carbon doping can enhance water adsorption/dissociation and CO_2 activation, and decrease energy barriers of forming hydrocarbon intermediates for C_2H_4, thus resulting in high selectivity of C_2H_4.